



LAWRENCE
LIVERMORE
NATIONAL
LABORATORY

Entire Plasmas can be Restructured when Electrons are Emitted from the Boundaries

M. D. Campanell

January 6, 2015

Physics of Plasmas

Disclaimer

This document was prepared as an account of work sponsored by an agency of the United States government. Neither the United States government nor Lawrence Livermore National Security, LLC, nor any of their employees makes any warranty, expressed or implied, or assumes any legal liability or responsibility for the accuracy, completeness, or usefulness of any information, apparatus, product, or process disclosed, or represents that its use would not infringe privately owned rights. Reference herein to any specific commercial product, process, or service by trade name, trademark, manufacturer, or otherwise does not necessarily constitute or imply its endorsement, recommendation, or favoring by the United States government or Lawrence Livermore National Security, LLC. The views and opinions of authors expressed herein do not necessarily state or reflect those of the United States government or Lawrence Livermore National Security, LLC, and shall not be used for advertising or product endorsement purposes.

Entire Plasmas can be Restructured when Electrons are Emitted from the Boundaries

M. D. Campanell

Lawrence Livermore National Laboratory, P.O. Box 808(L-630), Livermore, CA 94551, USA

It is well known that electron emission can restructure the thin sheaths at plasma-facing surfaces. But conventional models assume the plasma's structure negligibly changes (the "presheath" is still thought to be governed by ion acceleration to the Bohm speed). Here it is shown by theory and simulation that the presheath can take a fundamentally different structure where the emitted electrons entering the quasineutral region cause numerous changes. Gradients of total plasma density, ion and electron pressures, and electric potential throughout the presheath can carry different magnitudes, and opposite signs, from Bohm presheaths.

Plasma-wall interaction has a profound influence on the properties of bounded plasmas^{1,2}. The plasma's density and temperature are determined by the balance between ionization and heating versus the losses of charges and energy to the walls. Bombardment by ions can sputter away wall atoms, contaminating the plasma with impurities that radiate energy away^{2,3}. Sputtering is devastating for high temperature laboratory plasma applications including tokamaks. Plasma-surface interactions are also important for objects in space plasmas^{1,4}.

Plasma-facing walls usually charge negative because electrons have higher thermal velocities than ions. Ions then accelerate towards the wall and electrons get repelled. In equilibrium, the structure of a bounded symmetric planar plasma takes the form² sketched in Fig. 1(a). A classical sheath potential balances the losses of ions and electrons from the plasma. The sheath also serves to shield the charge on the wall. Although this nonneutral sheath region is thin, the acceleration of ions occurs through the entire quasineutral plasma, or "presheath", causing the plasma density to decrease from the midplane to the presheath-sheath edge². As recently reviewed by Robertson¹, the notions of sheath and presheath have been analyzed vigorously for almost a century since Tonks and Langmuir⁵. Various processes² are considered in theoretical plasma models including the ionization, heating, drag, and geometry for each application. In most models the assumption of ion acceleration to the Bohm velocity at the presheath edge is the main factor governing both the predicted plasma structure and the particle flows into the sheaths^{1,2,6,7}. Sheath theories are then used to set boundary conditions at the plasma edge. Because direct measurements of sheath and presheath structures are sparse in the literature⁸, most models are untested.

Secondary, thermionic and photon-induced electrons are emitted from surfaces in many laboratory and space plasmas. Important examples include fusion machines^{2,9}, dusty plasmas¹⁰, the moon¹¹, thrusters^{12,13}, RF discharges¹⁴, probe diagnostics¹⁵ and heated cathodes¹⁶. Emission alters the charge balance at a wall, thereby altering the sheath potential. When the emission coefficient γ , the ratio of emitted flux to the plasma electron influx, exceeds unity, some emission must return to the wall to keep zero current. The sheath is often assumed to take the "space charge

limited" (SCL) shape^{16,17,18,19} in Fig. 1(b). The potential profile $\phi(x)$ has a "dip" to suppress some emission, but the sheath potential is still negative; $\phi_{\text{wall}} - \phi_{\text{edge}} < 0$.

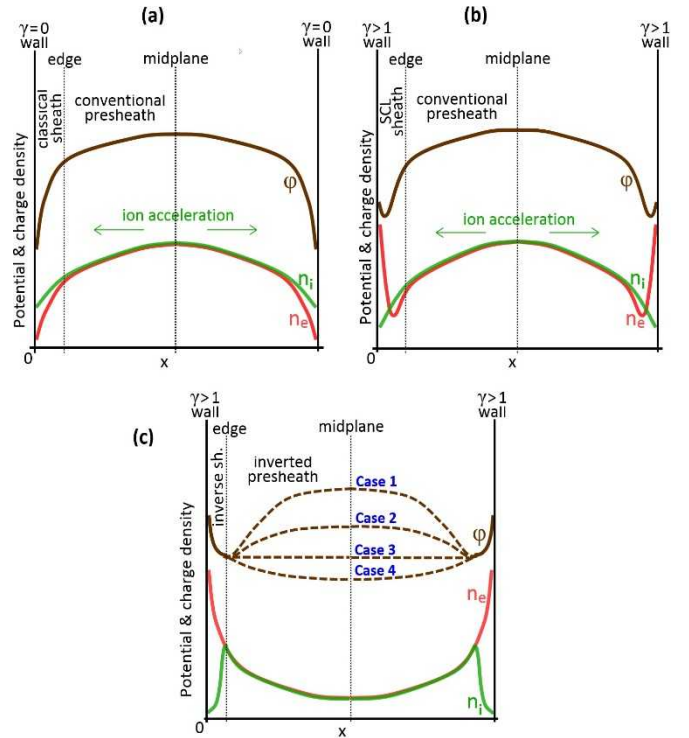


FIG. 1. Qualitative sketch of the potential and charge distributions in relative units in planar symmetric plasmas (a) without emission from the walls, (b) with strong emission in conventional theories, and (c) with strong emission in the state demonstrated in this paper. Sheath and presheath types are labeled in the left halfplane.

It is generally assumed that emission does not alter the presheath. Emitted electrons have a large spatial density at the wall, leading to a peak of n_e , Fig. 1(b). But acceleration by the negative sheath potential makes their density small at the sheath-presheath edge. Therefore regardless of how emitted electrons thermalize within the plasma, they do not alter the presheath physics. This conclusion is supported by rigorous theories. Ahedo's model of a plasma presheath and

sheath shows that even in SCL regimes, the density of emitted electrons at the presheath edge is only $\sim 10\%$ of the density of plasma electrons¹⁸. Emitted electrons do not significantly change the Bohm ion velocity either¹⁷.

Overall, a plasma's structure is predicted to be similar with or without emission from the boundaries, Fig. 1(a,b). However, this assumption must be revisited because recent works on sheaths with emission demonstrated an alternative solution where the sheath potential is *positive*^{20,21,22}, as sketched in Fig. 1(c). The basic idea is that when $\gamma > 1$, zero current can be maintained even if ions are confined in the plasma²¹. (If $T_i > 0$, some ions reach the wall anyway, but the solution still exists.) The structure of “inverse sheaths” was analyzed in Ref. 21. But the equally important issue not yet considered is, what will the plasma/presheath structure be in systems with strongly emitting boundaries?

In this paper, we show that plasmas with emitting boundaries can differ in numerous ways from conventional plasmas. The presheath density distribution $n(x)$ “inverts,” while $\phi(x)$ can take multiple shapes, see Fig. 1(c). A key underlying factor is that when the sheath potential is positive, the emitted electrons entering the plasma no longer have a low density but a high density. To demonstrate this, we assume the sheath is collisionless and that emitted electrons are half-Maxwellian with temperature T_{emit} . Because an inverse sheath retards the emission, the cold electrons entering the plasma from the edge are half-Maxwellian with $T_{\text{cold}} = T_{\text{emit}}$. Electrons at the edge moving towards the wall from the plasma interior we approximate as half-Maxwellian with temperature T_{hot} . These electrons get fully lost through the inverse sheath (none reflect back to the plasma). Because a half-Maxwellian² flux is $\sim nT^{1/2}$, the oppositely directed hot and cold electrons at the edge satisfy $n_{\text{cold}}T_{\text{cold}}^{1/2} \approx n_{\text{hot}}T_{\text{hot}}^{1/2}$ from the zero current condition (ion contribution to current balance can be neglected for this argument). Note this condition at the edge does not depend on γ at the wall. Overall, the partial densities of the hot and cold electrons at the edge have the relationship,

$$n_{\text{cold}} \approx n_{\text{hot}} \sqrt{\frac{T_{\text{hot}}}{T_{\text{emit}}}} \quad (1)$$

Because emitted electrons are much colder than plasma electrons in general²³, it follows from (1) that the emitted electrons dominate the total n_e at the quasineutral edge. This suggests n_{edge} exceeds whatever the hot plasma density is “upstream” (where any electrons that originated from the wall have been reheated to the plasma temperature). For a symmetric planar plasma with midplane temperature $T_{e,\text{mid}}$, the density ratio $n_{\text{edge}}/n_{\text{mid}}$ should scale roughly with $\sim (T_{e,\text{mid}}/T_{\text{emit}})^{1/2}$. Although precise calculation of presheath properties must include complicated analysis of heating, ionization and collisions, one can make some surprising general predictions starting with the plasma density

increasing towards strongly emitting surfaces as sketched in Fig. 1(c)!

In the rest of this paper, we further study “inverted plasmas” theoretically. We test the theory by simulating a bounded planar plasma with the rigorously verified electrostatic direct implicit particle-in-cell code²⁴ developed by D. Sydorenko. In past papers^{20,21,25,26,27}, important effects of emission on sheaths, transport and two stream instability were studied in simulations of low collisionality Hall plasmas where secondaries transited from wall to wall without altering the presheaths. Inverted presheaths are expected in systems where the emission remixes with the bulk plasma (a more common situation). Remixing could be from any combination of global electron heating, Coulomb interactions with hotter particles, or diffusion of electrons into and out of the near-surface region via other dimensions.

In Hall plasmas²⁵, electrons gain energy *parallel* to the walls (y-z plane) in a background $E \times B$ field, Fig. 2(a). Collisions with neutrals transfer some of this energy to the x-direction normal to the walls. We set $E_z = 350$ V/cm and $B_x = 100$ G. To make the plasmas collisional, we set (uniform xenon) gas density to $n_n = 4 \times 10^{21} \text{ m}^{-3}$ with plasma length $L = 3$ mm. Under these conditions, secondaries get reheated over x after elastic collisions with neutrals, rather than transit. The ionization collision cross section was adjusted to ensure volumetric ionization balances the wall charge losses. Coulomb interactions are insignificant here. Plasma densities are chosen so that the sheaths are smaller than the plasma yet large enough to be compared in a figure. In Fig. 2, distributions of potential, charge density and (x-directed) thermal energy are plotted for two representative runs. Because x-directed motion governs the presheath and sheath structures, we will analyze the 1D problem in x without discussing y-z plane motion. Thermal energy w is defined as the mean kinetic energy of particles at each x relative to the flow velocity v_{avg} . That is, $w \equiv \langle m(v_x - v_{\text{avg}})^2 \rangle / 2$, averaged over all particles. This metric is used instead of “temperature” because near the edges of bounded plasmas, charged particle velocity distributions are non-Maxwellian and a real temperature is undefined.

Simulation data shows that the charge densities increase towards the edges in Fig. 2(b,c), confirming the inverted plasma structure! Electrons at the midplane were verified to be almost Maxwellian, so we can write $T_{e,\text{mid}} \equiv 2\langle w_{e,\text{mid}} \rangle$. In Run A, $T_{e,\text{mid}} = 29$ eV from Fig. 2(f). The walls emit true secondaries with $T_{\text{emit}} = 2$ eV, but the “effective” T_{emit} well exceeds 2 eV because higher energy backscattered electrons are also present in the emission model²⁴. The density ratio $n_{\text{edge}}/n_{\text{mid}}$ is only 1.5 in Run A. For Run B, the emission yield was enhanced and all secondaries were set as “true” with $T_{\text{emit}} = 1$ eV. In Run B, $T_{e,\text{mid}} = 25$ eV, similar to Run A, but as predicted earlier, the smaller T_{emit} leads to a larger density ratio $n_{\text{edge}}/n_{\text{mid}} = 5$.

Note by comparison, conventional presheath theories¹ would predict $n(x)$ to *decrease* from the midplane to the edge by at least a factor of 2 regardless of any wall emission.

Conventional presheaths do appear in simulations with $\gamma < 1$ using this code^{25,27}.

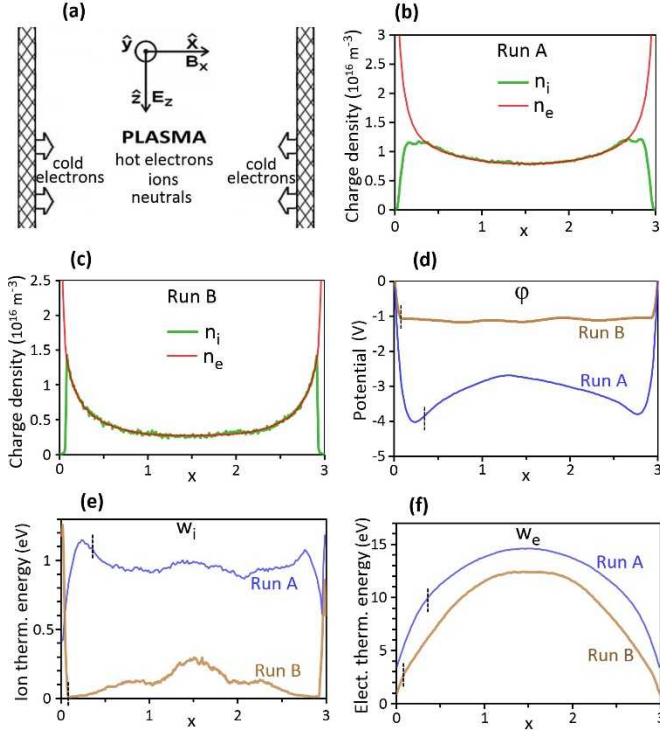


FIG. 2. (a) Simulation model. Charge densities between the walls in Run A (b) and Run B (c). Distributions of potential (d), ion thermal energy (e), and electron thermal energy (f) in both runs. The dashed lines in (d-f) mark the left sheath edge. Some notes: The peaks of w_i near the walls are insignificant because few ions can reach there. Flow velocities $v_{e,avg}$, $v_{i,avg}$ are negligible everywhere. The numerical grid is uniform and spaced small enough to ensure high resolution of sheaths and presheaths.

The plasma inverts because $\gamma > 1$ (1.7 in Run A and 2.2 in Run B). Inverse sheath theory²¹ predicts a positive sheath of amplitude $\Phi_{-1} \equiv \phi_{wall} - \phi_{edge} = T_{emit} \ln(\gamma)/q_e$. As expected, Φ_{-1} is larger in Run A (3.8V) than Run B (1.0V) due to the larger effective T_{emit} . However, no existing theory explains what $\phi(x)$ or $n(x)$ in the plasma should be. Run A may appear to show a conventional ion-accelerating presheath because the midplane potential ϕ_{mid} is above ϕ_{edge} . Yet the ions have negligible flow velocity in both runs! The E field actually forms due to ion *thermal* motion. The U-shaped $n(x)$ and almost uniform $w_i(x)$ in Run A combine to create a pressure force directed towards the midplane. An offsetting E field must form or else ions would accelerate inward!

To formally analyze the force balance, we use the 1D force equation for a charge species²,

$$mnv_{avg} \frac{dv_{avg}}{dx} = -\frac{dp}{dx} + qnE - F_{drag} \quad (2)$$

If $w_{i,edge} < q_e \Phi_{-1}$, few ions escape to the walls. The charge source needed for equilibrium can be neglected. The

net flow velocity $v_{i,avg}$ must be near zero everywhere. Therefore we can write $p_i = 2nw_i$. Velocity-dependent drag forces vanish. For ions, (2) reduces to

$$\frac{dp_i}{dx} = \frac{d}{dx}(2nw_i) = q_e nE. \quad (3)$$

It can now be shown that several $\phi(x)$ structures are possible in inverted plasmas, depending on ion temperature. Four cases are sketched in Fig. 1(c). When w_i is roughly uniform, there is an inward pressure force from (3) as explained earlier. To offset the pressure, $\phi(x)$ forms a “hill” ($\phi_{mid} > \phi_{edge}$). Depending how large w_i is, ϕ_{mid} could be above ϕ_{wall} (case 1) or below (case 2). Interestingly, a case 1 $\phi(x)$ measured experimentally could be misclassified as a Bohm presheath patched to an SCL sheath, c.f. Fig. 1(b). Other measurements such as $n(x)$ could distinguish the states. In Run A with $w_i \sim 1$ eV between the sheaths, $\phi(x)$ falls into case 2. In the cold ion limit, ion pressure vanishes and $\phi(x)$ is flat between the sheaths (case 3). This contrasts to conventional plasmas where a potential hill is always needed to accelerate ions even if $T_i = 0$ ^{6,8}. Case 4 is possible in systems where T_i is *nonuniform*, decreasing towards the walls. Depending how sharply w_i decreases, dp_i/dx in (3) can change sign, making $\phi(x)$ form a valley instead of a hill. Fig. 2(d) shows a small valley $\phi_{mid} - \phi_{edge} = -0.1$ V in Run B due to the $w_i(x)$ gradient. (Note, w_i in these simulations is thought to be governed by energy exchange with two-stream waves. The w_i was altered in Run B by enhancing i-n collisions to damp the waves. All data in Fig. 2 was time-averaged so that wave motions average to near zero, making the long term sheath/presheath structures clearer.)

The electrons also behave differently when a plasma is inverted. We predicted earlier that emitted electrons at the plasma edge would have (a) high partial density *and* (b) low energy, opposite to conventional presheath theory¹⁸. Therefore w_e drops sharply as n_e increases towards the edge, Fig. 2(f). Consider the force equation (2) for the electron species ($q \rightarrow -q_e$). The *net* electron flow velocity $v_{e,avg}$ must vanish to equal $v_{i,avg}$. Thus,

$$\frac{dp_e}{dx} = \frac{d}{dx}(2nw_e) = -q_e nE \quad (4)$$

In conventional presheaths, a p_e gradient always exists to accelerate electrons towards the wall with the ions². In the inverted plasma, a p_e gradient forms to offset whatever E field arose due to the ion thermal energy in (3). It could face either direction, or vanish in the cold ion limit. A global coupling between the plasma density and ion/electron pressures is found by combining (3) and (4),

$$n(w_e + w_i) = \text{const.} \quad (5)$$

Quantity (5) will conserve if the force balance behaves as theorized. Plotting $n_e(w_e + w_i)$ from both runs in Fig. 3, we see it is nearly constant except in the sheaths. Eq. (5) relied on our earlier assumption that no charge is lost, which was not exact in the runs but a good approximation (note $n_i(x)$ drops near zero at the walls). In systems with hotter ions ($w_{i,edge} > \sim q_e \Phi_{-1}$), more will escape. Flow velocities, charge sources and drags are needed to treat force balance. Still, many effects discussed here, like the increase of $n(x)$ towards the boundaries, will remain true. Any plasma in this regime will behave much differently from conventional predictions.

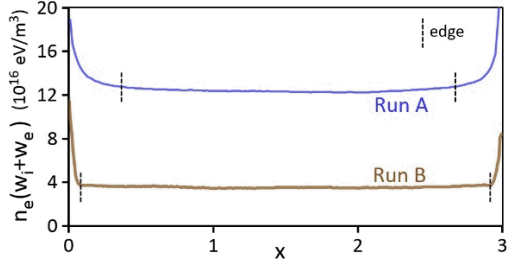


FIG. 3. Demonstration of the force balance in an inverted plasma. Conservation of $n_e(w_i + w_e)$ in the presheath region confirms Eq. (5).

Summary and Context – This paper showed that a fundamentally different plasma structure is possible near surfaces emitting a strong flux of electrons ($\gamma > 1$). The presheath is governed not by acceleration of ions but by other factors, leading to changes throughout the plasma. These results were not captured by previous theories. In the original Hobbs-Wesson paper¹⁷ and more recent studies of emission^{16,19,28}, the sheath structure was derived while *assuming* the presheath is conventional for all γ (ions have a strong flow velocity at the edge). Similarly, in existing fluid models for plasmas in systems such as tokamaks² and thrusters^{29,30}, the *sheath* transmission is adjusted with γ but conventional plasma equations are used (Bohm ion velocity sets the boundary condition).

Simulations here provided empirical evidence that inverted plasmas can exist. Other simulations of emission effects were conducted in the past^{16,23,31,32}. However most previous studies used “one-wall” models where plasma particles are injected across a source boundary, creating an artificial presheath called a source sheath²³. The two-wall simulations used here allowed presheaths to form in a natural way, closer to the situation in typical laboratory plasmas. Also, the remixing of emission in the plasma critical to inversion was not present in one-wall^{16,33,31} models, or in past two-wall^{13,20,21,27} simulations of collisionless plasmas.

Further experimental studies are now needed to confirm which sheath and presheath structures form near emitting boundaries. Although a few experiments exist on the subject¹, the structures were not known conclusively because spatial distributions of potential and charge like Fig. 1 are difficult to measure. Schwager *et al.*³³ measured ion impact energies at a thermionically emitting tungsten plate to

indirectly measure the potential difference between the plasma and plate. Predicting ion energies to be $\geq 1.7T_e$ from acceleration in a Bohm presheath and SCL sheath, the authors reported a “major discrepancy” that the measured energies were near zero! The discrepancy could be consistent with inverted plasma because any ions that reach the wall would impact with only their thermal energy. In addition, Table I of their paper indicates the plasma density was *larger* near the strongly emitting surface than upstream.

Besides restructuring the plasma, another way the presheath inversion would be important in applications is by limiting sputtering. In tokamaks for example, ion acceleration in the presheath and sheath usually increases impact energies by a few T_e , strongly enhancing sputtering². In an inverted state, erosion and impurity generation should be smaller, but changes to heat flux and plasma properties will occur too. Future studies should further investigate possible benefits and drawbacks of inversion. If heat flux can be mitigated by other methods^{34,35,36}, then perhaps emitting plates can be used on purpose to invert the plasma and reduce sputtering. Inversion might be possible even passively because secondary emission near the $\gamma = 1$ threshold was already reported possible in some divertor conditions^{9,37,38}. Thermionic emission from plasma-heated or externally heated metals including tungsten³³ is also intense. In future machines like ITER with higher plasma temperatures, both emissions could be intense depending on divertor operation.

Most of this work was performed under the auspices of the U.S. Department of Energy by Lawrence Livermore National Laboratory under Contract DE-AC52-07NA27344. Resources provided by the Princeton Plasma Physics Laboratory under DOE Contract No. DE-AC02-09CH11466, as well as the Walbridge Fund in the Princeton Environmental Institute at Princeton University were also used. This material is based upon work supported by the U.S. Department of Energy, Office of Science, Office of Fusion Energy Sciences.

- ¹ S. Robertson, Plasma Phys. Control. Fusion **55**, 093001 (2013).
- ² P. C. Stangeby, The Plasma Boundary of Magnetic Fusion Devices, Plasma Phys. Series (IOP, Bristol, 2000).
- ³ G. Federici, C. H. Skinner, J. N. Brooks, J. P. Coad, C. Grisolia, A. A. Haasz, A. Hassanein, V. Philipps, C. S. Pitcher, J. Roth, W. R. Wampler and D. G. Whyte, Nuclear Fusion **41**, 1967-2137 (2001).
- ⁴ E. C. Whipple, Rep. Prog. Phys. **44**, 1197-1250 (1981).
- ⁵ L. Tonks and I. Langmuir, Phys. Rev. **34**, 876-922 (1929).
- ⁶ K. U. Riemann, J. Phys. D: App. Phys. **24**, 493-518 (1991).
- ⁷ R. H. Cohen and D. D. Ryutov, Contrib. Plasma Phys. **44**, 111-25 (2004).
- ⁸ L. Oksuz and N. Hershkowitz, Phys. Rev. Lett. **89**, 145001 (2002).
- ⁹ J. P. Gunn, Plasma Phys. Controlled Fusion **54**, 085007 (2012).
- ¹⁰ G. L. Delzanno and X. Tang, Phys. Rev. Lett. **113**, 035002 (2014).
- ¹¹ J. Halekas, G. T. Delory, R. P. Lin, T. J. Stubbs and W. M. Farrell, Planetary and Space Science **57**, 78-82 (2009).
- ¹² Y. Raitses, I. D. Kaganovich, A. Khrabrov, D. Sydorenko, N. J. Fisch, and A. Smolyakov, IEEE Trans. Plasma Sci. **39**, 995-1006 (2011).
- ¹³ F. Taccogna, S. Longo, M. Capitelli, and R. Schneider, Contrib. Plasma Phys. **48**, 375 (2008).
- ¹⁴ R. Flohr and A. Piel, Phys. Rev. Lett. **70**, 1108 (1993).
- ¹⁵ C. Ionita, J. Grünwald, Ch. Maszl, R. Stärz, M. Čerček, B. Fonda, T. Gyergyek, G. Filipič, J. Kovačič, C. Silva, H. Figueiredo, T. Windisch, O. Grulke, T. Klinger, and R. Schrittwieser, Contrib. Plasma Phys. **51**, 264-270 (2011).
- ¹⁶ J.P. Sheehan, N. Hershkowitz, I. D. Kaganovich, H. Wang, Y. Raitses, E. V. Barnat, B. R. Weatherford and D. Sydorenko, Phys. Rev. Lett. **111**, 075002 (2013).
- ¹⁷ G. D. Hobbs and J. A. Wesson, Plasma Phys. **9**, 85-87 (1967).
- ¹⁸ E. Ahedo, Phys. Plasmas **9**, 4340-4347 (2002).
- ¹⁹ J. Seon, E. Lee, W. Choe and H. J. Lee, Curr. Appl. Phys. **12**, 663-667 (2012).
- ²⁰ M. D. Campanell, A. V. Khrabrov and I. D. Kaganovich, Phys. Rev. Lett. **108**, 255001 (2012).
- ²¹ M. D. Campanell, Phys. Rev. E. **88**, 033103 (2013).
- ²² F. Taccogna, Eur. Phys. J. D **68**:199 (2014).
- ²³ L. A. Schwager, Phys. Fluids B **5**, 631-645 (1993).
- ²⁴ D. Sydorenko, Ph.D. thesis, University of Saskatchewan, 2006.
- ²⁵ I. D. Kaganovich, Y. Raitses, D. Sydorenko and A. Smolyakov, Phys. Plasmas **14**, 057104 (2007).
- ²⁶ D. Sydorenko, A. Smolyakov, I. D. Kaganovich and Y. Raitses, Physics of Plasmas **14**, 013508 (2007).
- ²⁷ D. Sydorenko, I. Kaganovich, Y. Raitses and A. Smolyakov, Phys. Rev. Lett. **103**, 145004 (2009).
- ²⁸ A. I. Morozov and V. V. Savel'ev, Plasma Phys. Rep. **33**, 20 (2007).
- ²⁹ K. Hara, M. J. Sekerak and I. D. Boyd and A. D. Gallimore, J. Appl. Phys. **115**, 203304 (2014).
- ³⁰ E. Ahedo and V. De Pablo, Phys. Plasmas **14**, 083501 (2007).
- ³¹ F. Taccogna, S. Longo and M. Capitelli, Phys. Plasmas **11**, 1220-1228 (2004).
- ³² T. Gyergyek and J. Kovačič, Physics of Plasmas **19**, 013506 (2012).
- ³³ L. A. Schwager, W. L. Hsu and M. D. Tung, Phys. Fluids B **5**, 621-630 (1993).
- ³⁴ J. Li, H. Y. Guo, B. N. Wan, X. Z. Gong, Y. F. Liang, G. S. Xu, K. F. Gan, J. S. Hu, H. Q. Wang, L. Wang, et al., Nature Physics **9**, 817-821 (2013).
- ³⁵ S. J. Zweben, M. D. Campanell, B. C. Lyons, R. J. Maqueda, Y. Raitses, A. L. Roquemore, F. Scotti and H. Takahashi, Plasma Phys. Control. Fusion **54**, 105012 (2012).
- ³⁶ D. D. Ryutov, R. H. Cohen, T. D. Rognlien and M. V. Umansky, Plasma Phys. Control. Fusion **54**, 124050 (2012).
- ³⁷ E. Oyarzabal, A. B. Martin-Rojo and F. L. Tabarés, J. Nuc. Mat. **452**, 37-40 (2014).
- ³⁸ R. A. Pitts and G. F. Matthews, J. Nucl. Mater. **176**, 877-882 (1990).